

Pinning down $|\Delta c| = |\Delta u| = 1$ couplings with rare charm baryon decays

Marcel Golz,^{*} Gudrun Hiller,[†] and Tom Magorsch[‡]

*TU Dortmund University, Department of Physics,
Otto-Hahn-Str.4, D-44221 Dortmund, Germany*

We study the full angular distribution of semileptonic rare charm baryon decays in which the secondary baryon undergoes weak decay with sizable polarization parameter, $\Xi_c^+ \rightarrow \Sigma^+ (\rightarrow p\pi^0)\ell^+\ell^-$, $\Xi_c^0 \rightarrow \Lambda^0 (\rightarrow p\pi^-)\ell^+\ell^-$ and $\Omega_c^0 \rightarrow \Xi^0 (\rightarrow \Lambda^0\pi^0)\ell^+\ell^-$. Such self-analyzing decay chains allow for seven additional observables compared to three-body decays such as $\Lambda_c \rightarrow p\ell^+\ell^-$, with different sensitivities to the $|\Delta c| = |\Delta u| = 1$ weak couplings. Opportunities to test the standard model in $c \rightarrow u$ transitions with standard model null tests and other angular observables are worked out. We show that a joint model-independent analysis of the leptonic A_{FB}^ℓ , hadronic A_{FB}^H , and combined forward-backward asymmetry $A_{\text{FB}}^{\ell H}$ together with the fraction of longitudinally produced leptons, F_L , is able to pin down the dipole couplings C_7, C_7' and the semileptonic (axial-) vector ones C_{10}, C_9, C_{10}' . A_{FB}^H is also accessible with dineutrino $c \rightarrow u\nu\bar{\nu}$ modes and probes right-handed currents.

I. INTRODUCTION

Flavor changing neutral currents of charm quarks are strongly suppressed in the standard model (SM) by an efficient Glashow-Iliopoulos-Maiani (GIM) mechanism. At the same time sizable resonance contributions shadow new physics (NP) in simple observables such as branching ratios of semileptonic $c \rightarrow u\ell^+\ell^-$ -induced modes [1]. This very GIM suppression, on the other hand, along with approximate symmetries of the SM gives directions for clean observables and null tests, which probe a broad range of NP phenomena. Corresponding SM tests with $|\Delta c| = |\Delta u| = 1$ transitions complement beyond standard model (BSM) searches with strange and beauty quark processes and provide novel and unique insights into flavor from the up-quark sector. Several opportunities to test the SM have been worked out for D -meson decays, *e.g.* [2–8].

Rare semileptonic decays of charm baryons have been explored as a NP probe recently [9–12]. In [12] we analyzed the NP sensitivity of rare semileptonic decays of Λ_c , Ξ_c and Ω_c -baryons, here collectively denoted by $B_0 \rightarrow B_1\ell^+\ell^-$ with the initial (daughter) baryon denoted by $B_0(B_1)$, see

^{*}Electronic address: marcel.golz@tu-dortmund.de

[†]Electronic address: ghiller@physik.uni-dortmund.de

[‡]Electronic address: tom.magorsch@tu-dortmund.de

TABLE I: Self-analyzing rare charm four-body decays $B_0 \rightarrow B_1(\rightarrow B_2\pi)\ell^+\ell^-$ and information on the branching ratios and weak decay parameters α of the secondary baryonic $B_1 \rightarrow B_2\pi$ decay [16].

	$\Xi_c^+ \rightarrow \Sigma^+ (\rightarrow p\pi^0)\ell^+\ell^-$	$\Xi_c^0 \rightarrow \Lambda^0 (\rightarrow p\pi^-)\ell^+\ell^-$	$\Omega_c^0 \rightarrow \Xi^0 (\rightarrow \Lambda^0\pi^0)\ell^+\ell^-$
$\mathcal{B}(B_1 \rightarrow B_2\pi)$	$51.6 \pm 0.3\%$	$63.9 \pm 0.5\%$	$99.5 \pm 0.0\%$
α	-0.98 ± 0.01	0.73 ± 0.01	-0.36 ± 0.01

[10] for dineutrino modes $B_0 \rightarrow B_1\nu\bar{\nu}$. In this work we consider (quasi-) four-body decays, where the B_1 further decays weakly to a hyperon B_2 and a pion. Since kinematic observables, such as the direction of the B_2 momentum, provide information on the spin of the decaying B_1 baryon, these channels are termed 'self-analyzing'. Advantages of such modes for NP searches are well-known in b -physics, notably using $\Lambda(1116) \rightarrow p\pi$ in rare decays of Λ_b -baryons, see for instance Ref. [13–15].

In charm, we identify the following decay channels suitable for polarization studies,

$$\begin{aligned} \Xi_c^+ \rightarrow \Sigma^+ (\rightarrow p\pi^0)\ell^+\ell^-, \quad \Xi_c^0 \rightarrow \Lambda^0 (\rightarrow p\pi^-)\ell^+\ell^-, \quad \Omega_c^0 \rightarrow \Xi^0 (\rightarrow \Lambda^0\pi^0)\ell^+\ell^-, \\ \Xi_c^+ \rightarrow \Sigma^+ (\rightarrow p\pi^0)\nu\bar{\nu}, \quad \Xi_c^0 \rightarrow \Lambda^0 (\rightarrow p\pi^-)\nu\bar{\nu}, \quad \Omega_c^0 \rightarrow \Xi^0 (\rightarrow \Lambda^0\pi^0)\nu\bar{\nu}, \end{aligned}$$

since Σ^+ , Λ^0 and Ξ^0 are self-analyzing, with sizable decay parameter α (we do not consider $\Sigma^0 \rightarrow \Lambda\gamma$). The branching ratios and decay parameters of the secondary baryon decays are provided in Tab. I. Our aim is to work out null tests and to complement $|\Delta c| = |\Delta u| = 1$ analyses of charmed meson decays, *e.g.* [6, 7].

Requisite vector and tensor form factors for $\Lambda_c \rightarrow p$ transitions have been computed on the lattice [9] and in quark models [17], and for $\Xi_c \rightarrow \Sigma$ from Light cone sum rules [18]. As in [12], we employ $\Lambda_c \rightarrow p$ lattice form factors [9] and relate them to the Ξ_c, Ω_c ones using $SU(3)_F$ -flavor symmetries, if applicable. This procedure is improvable with better knowledge of the form factors, however, to explore NP signals in SM null tests a precise knowledge of form factors is not essential.

None of the rare charm baryon modes has been observed so far, but the upper limit on the $\Lambda_c \rightarrow p\mu^+\mu^-$ branching ratio at $\sim 10^{-7}$ by LHCb [19] is close to the estimated size of the resonance contributions [12]. Limits on $\Lambda_c \rightarrow pe^+e^-$ and lepton flavor violating ones $\Lambda_c \rightarrow pe^\pm\mu^\mp$ are at the level of $\sim 10^{-5}$ by BaBar [20]. Semileptonic rare charm baryon decays are suitable for study at high luminosity flavor facilities, such as LHCb [21], Belle II [22], BES III [23], and possible future machines [24, 25].

The plan of the paper is as follows: In Sec. II we discuss exclusive rare charm baryon decay modes within a low energy effective field theory (EFT) framework, including phenomenological resonance contributions. We also present the full angular distribution for four-body baryon decays

and review some of the simpler observables already accessible with three-body decays. We work out the impact of the new null tests and other clean NP probes in Sec. III, and give an early stage strategy to disentangle NP Wilson coefficients. In Sec. IV we present further null tests, based on more advanced angular observables, with decays into dineutrinos and for decays of polarized charm baryons. We conclude in Sec. V. We present the helicity amplitudes in terms of Wilson coefficients and form factors in App. A, and provide details on the helicity amplitude description of the secondary weak decay in App. B. In App. C we give the full angular distribution for initially polarized baryon decays.

II. THEORY OF $|\Delta c| = |\Delta u| = 1$ FOUR-BODY BARYON DECAYS

We give general formulae for semileptonic rare charm baryon decays in the SM and beyond. In Sec. II A we introduce the weak Hamiltonian at the charm mass scale and discuss SM contributions. The fully differential distribution for the (quasi-)four-body decay of unpolarized charmed baryons is presented in Sec. II B.

A. An effective field theory approach to charm physics

Consider the weak effective Hamiltonian for $c \rightarrow u\ell^+\ell^-$ transitions

$$\mathcal{H}_{\text{eff}} \supset -\frac{4G_F \alpha_e}{\sqrt{2} 4\pi} \sum_{k=7,9,10} (C_k O_k + C'_k O'_k), \quad (1)$$

where α_e and G_F denote the fine structure and Fermi's constant, respectively. The dimension six operators are given as

$$\begin{aligned} O_7 &= \frac{m_c}{e} (\bar{u}_L \sigma_{\mu\nu} c_R) F^{\mu\nu}, & O'_7 &= \frac{m_c}{e} (\bar{u}_R \sigma_{\mu\nu} c_L) F^{\mu\nu}, \\ O_9 &= (\bar{u}_L \gamma_\mu c_L) (\bar{\ell} \gamma^\mu \ell), & O'_9 &= (\bar{u}_R \gamma_\mu c_R) (\bar{\ell} \gamma^\mu \ell), \\ O_{10} &= (\bar{u}_L \gamma_\mu c_L) (\bar{\ell} \gamma^\mu \gamma_5 \ell), & O'_{10} &= (\bar{u}_R \gamma_\mu c_R) (\bar{\ell} \gamma^\mu \gamma_5 \ell), \end{aligned} \quad (2)$$

with the electromagnetic field strength tensor $F^{\mu\nu}$, the chiral projectors $L = (1 - \gamma_5)/2$, $R = (1 + \gamma_5)/2$ and $\sigma^{\mu\nu} = \frac{i}{2} [\gamma^\mu, \gamma^\nu]$. For the mass of the charm quark we use $m_c(m_c) = 1.27$ GeV, in the $\overline{\text{MS}}$ mass scheme. SM contributions to the coefficients of the operators in Eq. (1) arise from four-quark operators at the W -mass scale and from intermediate resonances M , decaying electromagnetically to dileptons, as in the quasi four-body decay chain $B_0 \rightarrow B_1 M (\rightarrow \ell^+ \ell^-) \rightarrow B_1 \ell^+ \ell^- \rightarrow B_1 (\rightarrow B_2 \pi) \ell^+ \ell^- \rightarrow B_2 \pi \ell^+ \ell^-$. Note, the lifetime of the resonances $M = \omega, \rho, \phi$ is

TABLE II: Resonance parameters a_ω, a_ϕ defined in (3) for various rare charm baryon transitions, see text.

	$\Lambda_c \rightarrow p$	$\Xi_c^+ \rightarrow \Sigma^+$	$\Xi_c^0 \rightarrow \Lambda^0$	$\Omega_c^0 \rightarrow \Xi^0$
a_ω	0.062 ± 0.009	~ 0.06	~ 0.06	~ 0.05
a_ϕ	0.110 ± 0.008	~ 0.1	~ 0.1	~ 0.09

much shorter than the one of the daughter baryons $B_1 = \Sigma^+, \Lambda, \Xi^0$, which decay weakly after the dileptons have been produced. The resonance contributions are taken into account with a phenomenological ansatz, as

$$C_9^R(q^2) = a_\omega e^{i\delta_\omega} \left(\frac{1}{q^2 - m_\omega^2 + im_\omega\Gamma_\omega} - \frac{3}{q^2 - m_\rho^2 + im_\rho\Gamma_\rho} \right) + \frac{a_\phi e^{i\delta_\phi}}{q^2 - m_\phi^2 + im_\phi\Gamma_\phi}, \quad (3)$$

implying a contribution to O_9 . Here, m_M and Γ_M denote the mass and total width of the meson M . The strong phases δ_M are unknown and provide a significant amount of theoretical uncertainty. We neglect effects from intermediate η, η' mesons as they are strongly localized and have a negligible effect on the (differential) branching ratio [12]. We further use isospin to relate the ρ and ω contributions [26], as no data on any of the $B_0 \rightarrow B_1\rho$ branching ratios is available. Experimental input on the parameters a_M is provided in Tab. II. Note that due to Belle's recent measurement of $\mathcal{B}(\Lambda_c^+ \rightarrow p\omega)$ [27] the corresponding entry slightly differs from the one in [12].

For the form factors we use the same helicity-based definition as in [9, 12]. Form factors from lattice computations for $\Lambda_c \rightarrow p$ transitions are obtained in Ref. [9]. We obtain the form factors for the baryon transitions studied in this work via flavor symmetries, see Refs. [12, 28] for details. Consequently, we find for any of the ten form factors commonly denoted here as $f_{B_0 \rightarrow B_1}$

$$f_{\Lambda_c \rightarrow p} = f_{\Xi_c^+ \rightarrow \Sigma^+} = \sqrt{6} f_{\Xi_c^0 \rightarrow \Lambda^0} \simeq f_{\Omega_c^0 \rightarrow \Xi^0}. \quad (4)$$

We emphasize that all but the last relation follow from $SU(3)_F$ symmetry. The connection to the Ω_c is broken as it sits in a different multiplet. In absence of form factor determinations for the latter at the same level as those for the $\Lambda_c \rightarrow p$ we use this simple relation to be able to make progress. We stress that this ansatz does not affect the null test features discussed in this work. The relations (4) have also been used for $B_0 \rightarrow B_1(\phi, \omega)$ to obtain the a_M factors for the decays other than $\Lambda_c \rightarrow p(\phi, \omega)$ presented in Tab. II. Specifically, the $\Lambda_c^+ \rightarrow p$ parameters serve as an input to all other modes, as branching ratio data for the latter are not available. An exception is $\mathcal{B}(\Xi_c^0 \rightarrow \Lambda^0\phi) = (4.9 \pm 1.5) \times 10^{-4}$ [29], which gives $a_\phi = 0.080 \pm 0.013$, consistent with the value in Tab. II.

Due to the severe GIM cancellation in rare charm decays, the perturbative SM contributions are overwhelmed by the effects from intermediate resonances: Perturbatively, $C_7^{\text{eff}}(q^2) \sim 10^{-3}$,

$C_9^{\text{eff}}(q^2) \sim 10^{-2}$, whereas the ρ , ω , ϕ resonances yield $C_9^R(q^2) \sim \mathcal{O}(10)$ on resonance peaks and $\sim \mathcal{O}(1)$ off peak, see [12], based on results in [5, 30, 31]. The primed Wilson coefficients of (2) are suppressed by m_u/m_c and are negligible in the SM. The Wilson coefficient C_{10} vanishes in the SM, and therefore leptonic axialvector currents do, too, providing a prime opportunity for null test searches in charm. Electromagnetic loop contributions to the matrix element of 4-quark operators, or mixing, induce contributions not exceeding permille level [6].

B. Fully differential distribution for $m_\ell \neq 0$

We present the full differential decay distribution for four-body decays $B_0 \rightarrow B_1(\rightarrow B_2\pi)\ell^+\ell^-$. A brief discussion of $B_0 \rightarrow B_1(\rightarrow B_2\pi)\nu\bar{\nu}$ decays is deferred to Sec. IV B. We compute the distribution using the helicity formalism [32, 33] for unpolarized charmed baryons and keeping finite lepton masses, $m_\ell \neq 0$. Details on the helicity amplitudes are given in App. A. To be specific, expressions are given for the decay $\Xi_c^+ \rightarrow \Sigma^+(\rightarrow p\pi^0)\ell^+\ell^-$, however, with replacements of masses, form factors and $B_1 \rightarrow B_2\pi$ branching ratios, the same holds for any of the other modes in Tab. I. The fully differential distribution can be parameterized in terms of the ten q^2 -dependent angular observables $K_i = K_i(q^2)$ as

$$\begin{aligned} \frac{d^4\Gamma}{dq^2 d\cos\theta_\ell d\cos\theta_\pi d\phi} = \frac{3}{8\pi} \cdot \left[& K_{1ss} \sin^2\theta_\ell + K_{1cc} \cos^2\theta_\ell + K_{1c} \cos\theta_\ell \right. \\ & + (K_{2ss} \sin^2\theta_\ell + K_{2cc} \cos^2\theta_\ell + K_{2c} \cos\theta_\ell) \cos\theta_\pi \\ & + (K_{3sc} \sin\theta_\ell \cos\theta_\ell + K_{3s} \sin\theta_\ell) \sin\theta_\pi \sin\phi \\ & \left. + (K_{4sc} \sin\theta_\ell \cos\theta_\ell + K_{4s} \sin\theta_\ell) \sin\theta_\pi \cos\phi \right]. \end{aligned} \quad (5)$$

Here, θ_ℓ is the angle of the ℓ^+ with respect to the negative direction of flight of the charmed baryon (Ξ_c^+) in the dilepton rest frame. Similarly, θ_π is the angle between the momentum of the final state (B_2)baryon (p) and the negative direction of flight of the B_1 baryon (Σ^+) in the proton-pion center-of-mass frame. The azimuthal angle ϕ describes the angle between the dilepton and the $p\pi^0$ decay planes. The allowed regions for the angles θ_ℓ , θ_π , ϕ are $-1 \leq \cos\theta_\ell \leq +1$, $-1 < \cos\theta_\pi < 1$ and $0 < \phi < 2\pi$.

The q^2 -dependent coefficients K_i are given as [14]¹

$$\begin{aligned}
\frac{K_{1ss}}{\mathcal{B}(\Sigma^+ \rightarrow p\pi^0)} &= q^2 v^2 \left(\frac{1}{2} U^{11+22} + L^{11+22} \right) + 4m_\ell^2 (U^{11} + L^{11} + S^{22}), \\
\frac{K_{1cc}}{\mathcal{B}(\Sigma^+ \rightarrow p\pi^0)} &= q^2 v^2 U^{11+22} + 4m_\ell^2 (U^{11} + L^{11} + S^{22}), \\
\frac{K_{1c}}{\mathcal{B}(\Sigma^+ \rightarrow p\pi^0)} &= -2q^2 v P^{12}, \\
\frac{K_{2ss}}{\mathcal{B}(\Sigma^+ \rightarrow p\pi^0) \cdot \alpha} &= q^2 v^2 \left(\frac{1}{2} P^{11+22} + L_P^{11+22} \right) + 4m_\ell^2 (P^{11} + L_P^{11} + S_P^{22}), \\
\frac{K_{2cc}}{\mathcal{B}(\Sigma^+ \rightarrow p\pi^0) \cdot \alpha} &= q^2 v^2 P^{11+22} + 4m_\ell^2 (P^{11} + L_P^{11} + S_P^{22}), \\
\frac{K_{2c}}{\mathcal{B}(\Sigma^+ \rightarrow p\pi^0) \cdot \alpha} &= -2q^2 v U^{12}, \\
\frac{K_{3sc}}{\mathcal{B}(\Sigma^+ \rightarrow p\pi^0) \cdot \alpha} &= -2\sqrt{2} q^2 v^2 I_2^{11+22}, \\
\frac{K_{3s}}{\mathcal{B}(\Sigma^+ \rightarrow p\pi^0) \cdot \alpha} &= 4\sqrt{2} q^2 v I_{4P}^{12}, \\
\frac{K_{4sc}}{\mathcal{B}(\Sigma^+ \rightarrow p\pi^0) \cdot \alpha} &= 2\sqrt{2} q^2 v^2 I_{1P}^{11+22}, \\
\frac{K_{4s}}{\mathcal{B}(\Sigma^+ \rightarrow p\pi^0) \cdot \alpha} &= -4\sqrt{2} q^2 v I_3^{12},
\end{aligned} \tag{6}$$

in agreement with our own computation and [34]. Here, $v = \sqrt{1 - \frac{4m_\ell^2}{q^2}}$, $U^{11+22} = U^{11} + U^{22}$ and likewise for L, P, I_{1P}, I_2 . The q^2 -dependent terms U, L, S, P, L_P, S_P denote quadratic expressions of helicity amplitudes and correspond to unpolarized transverse, longitudinal, scalar, transverse parity-odd, longitudinal parity-odd and scalar parity-odd contributions, respectively. The coefficients I_{1P}, I_{4P} and I_2, I_3 correspond to longitudinal-transverse interference terms, where the subscript P refers to the parity-odd ones. We refer to App. A for expressions in terms of Wilson coefficients and hadronic form factors, $f_i(q^2), g_i(q^2), i = +, \perp, 0$ and $h_j(q^2), \tilde{h}_j(q^2), j = +, \perp$, which are defined in Ref. [9, 12].

The GIM mechanism is responsible for the absence of leptonic axial-vector currents in rare charm decays. Therefore, neglecting higher order electromagnetic contributions to C_{10} [6],

$$K_{1c}^{\text{SM}} = K_{2c}^{\text{SM}} = K_{3s}^{\text{SM}} = K_{4s}^{\text{SM}} = 0. \tag{7}$$

At the same time, these angular observables serve as clean null tests of the SM. The first one, K_{1c} , has already been studied in $\Lambda_c \rightarrow p\mu^+\mu^-$ [9] and three-body $1/2 \rightarrow 1/2\ell^+\ell^-$ decays of Λ_c, Ξ_c and

¹ We adapt the notation of helicity expressions $I_{iP}^{mm'}$, $i = 1, 2, 3, 4$ from [14], however use them to formulate angular observables in a notation similar to [15]. Note that we dropped the subscript P from $I_2^{mm'}$, $I_3^{mm'}$ since these two interference terms are parity-even.

Ω_c 's [12]. The other three null tests, K_{2c} , K_{3s} and K_{4s} are a new result of this work. They become accessible in four-body decays, and vanish for $\alpha = 0$. We analyze the NP sensitivity in Section III.

Let us recap basic features of the distribution Eq. (5). If both θ_π and ϕ are not measured, only the first line survives and one recovers the double differential distribution for three-body decays:

$$\frac{d^2\Gamma}{dq^2 d\cos\theta_\ell} = \int_{-1}^1 \int_0^{2\pi} \frac{d^4\Gamma}{dq^2 d\cos\theta_\ell d\cos\theta_\pi d\phi} d\phi d\cos\theta_\pi = \frac{3}{2} (K_{1ss} \sin^2\theta_\ell + K_{1cc} \cos^2\theta_\ell + K_{1c} \cos\theta_\ell). \quad (8)$$

From here follows the q^2 -differential decay rate

$$\frac{d\Gamma}{dq^2} = \int_{-1}^1 \frac{d^2\Gamma}{dq^2 d\cos\theta_\ell} d\cos\theta_\ell = 2K_{1ss} + K_{1cc}, \quad (9)$$

the longitudinal fraction of the dilepton system, F_L ,

$$F_L = \frac{2K_{1ss} - K_{1cc}}{2K_{1ss} + K_{1cc}}, \quad (10)$$

and the forward-backward asymmetry of the leptonic scattering angle, A_{FB}^ℓ ,

$$A_{\text{FB}}^\ell = \frac{1}{d\Gamma/dq^2} \left[\int_0^1 - \int_{-1}^0 \right] \frac{d^2\Gamma}{dq^2 d\cos\theta_\ell} d\cos\theta_\ell = \frac{3}{2} \frac{K_{1c}}{2K_{1ss} + K_{1cc}}, \quad (11)$$

see [12] for a detailed discussion of the phenomenology in and beyond the SM.

Kinematic endpoints are $q_{\text{min}}^2 = 4m_\ell^2$, corresponding to maximum hadronic recoil, and $q_{\text{max}}^2 = (m_{B_0} - m_{B_1})^2$, corresponding to zero hadronic recoil. The latter is subject to symmetry relations, enforcing $K_{1ss} = K_{1cc}$, hence $F_L = 1/3$ and similarly $K_{2ss} = K_{2cc}$ model-independently at this point [35]. These relations hold also at the other end of the spectrum, at q_{min}^2 , because here the four-momenta of the leptons coincide which leads also to a reduction of Lorentz structures [12].

The integrated decay rate is obtained as

$$\Gamma = \int_{q_{\text{min}}^2}^{q_{\text{max}}^2} (2K_{1ss} + K_{1cc}) dq^2, \quad (12)$$

where phase space cuts may be applied. Integrating the full q^2 region with ± 40 MeV cuts [19] around the ω and the ϕ resonances, we find

$$\begin{aligned} \mathcal{B}(\Xi_c^+ \rightarrow \Sigma^+(\rightarrow p\pi^0)\mu^+\mu^-) &\sim 1.8 \times 10^{-8}, \\ \mathcal{B}(\Xi_c^0 \rightarrow \Lambda^0(\rightarrow p\pi^-)\mu^+\mu^-) &\sim 2.4 \times 10^{-9}, \\ \mathcal{B}(\Omega_c^0 \rightarrow \Xi^0(\rightarrow \Lambda^0\pi^0)\mu^+\mu^-) &\sim 2.5 \times 10^{-8}, \end{aligned} \quad (13)$$

in agreement with results in Ref. [12] multiplied with $\mathcal{B}(B_1 \rightarrow B_2\pi)$ given in Tab. I.

III. PROBING NP WITH ANGULAR OBSERVABLES

In this section we discuss angular observables in rare, semileptonic charm baryon decays that can cleanly signal NP, and work out sensitivities to specific Wilson coefficients. The full angular distribution (5) features four GIM-based null tests, K_{1c}, K_{2c}, K_{3s} and K_{4s} , which vanish in the SM (7). In addition, F_L (10) is also a sensitive probe of NP [12]. In Sec. III A we work out BSM signatures in F_L and in a similarly simple and sensitive observable, the hadronic forward-backward asymmetry, $\sim 2K_{2ss} + K_{2cc}$. K_{1c} and K_{2c} correspond to the leptonic and combined leptonic-hadronic forward-backward asymmetries, respectively. They are discussed in Sec. III B. Null tests in the longitudinal-transverse interference terms $K_{4s} \sim I_3^{12}$ and $K_{3s} \sim I_{4P}^{12}$ are analyzed in the next Sec. IV. We summarize a strategy to disentangle Wilson coefficients based on three asymmetries and F_L in Sec. III C.

A. A_{FB}^{H} and F_L

The hadronic forward-backward asymmetry A_{FB}^{H} is defined similar to the leptonic one, A_{FB}^{ℓ} , Eq. (11), as

$$\begin{aligned} A_{\text{FB}}^{\text{H}} &= \frac{1}{d\Gamma/dq^2} \left[\int_0^1 - \int_{-1}^0 \right] \int_{-1}^1 \int_0^{2\pi} \frac{d^4\Gamma}{dq^2 d\cos\theta_\ell d\cos\theta_\pi d\phi} d\phi d\cos\theta_\ell d\cos\theta_\pi \\ &= \frac{1}{2} \frac{2K_{2ss} + K_{2cc}}{2K_{1ss} + K_{1cc}}. \end{aligned} \quad (14)$$

Unlike A_{FB}^{ℓ} , A_{FB}^{H} is not a null test of the SM, however, it turns out to be a highly sensitive probe of right-handed quark currents as illustrated in the left plot of Fig. 1. Here, the orange curve displays the SM expectation, and several NP benchmarks are shown in red, green and blue. The brackets in the subscripts are understood as *or*, for instance, $C'_{9,(10)} = 0.5$ is short for $C'_9 = 0.5$ *or* $C'_{10} = 0.5$. We learn that A_{FB}^{H} is sensitive to C'_7 , C'_9 and C'_{10} .

A_{FB}^{H} shares features with F_L (10), shown in the right plot of Fig. 1: Cancellation of hadronic uncertainties in the SM (orange), strong sensitivity to NP contributions in *some* Wilson coefficients and large uncertainties in NP scenarios due to unknown strong phases, observed previously for F_L in [12]. The main differences between these two angular observables are the following:

- $F_L = 1/3$ at both kinematic endpoints of maximum and zero recoil, whereas A_{FB}^{H} is unconstrained at low q^2 and vanishes at maximum q^2 .
- F_L is mostly sensitive to radiative dipole couplings C_7 and C'_7 , see the blue and green bands in the right plot of Fig. 1. A_{FB}^{H} is similar (equal) to the SM in scenarios involving C_7 or C_9

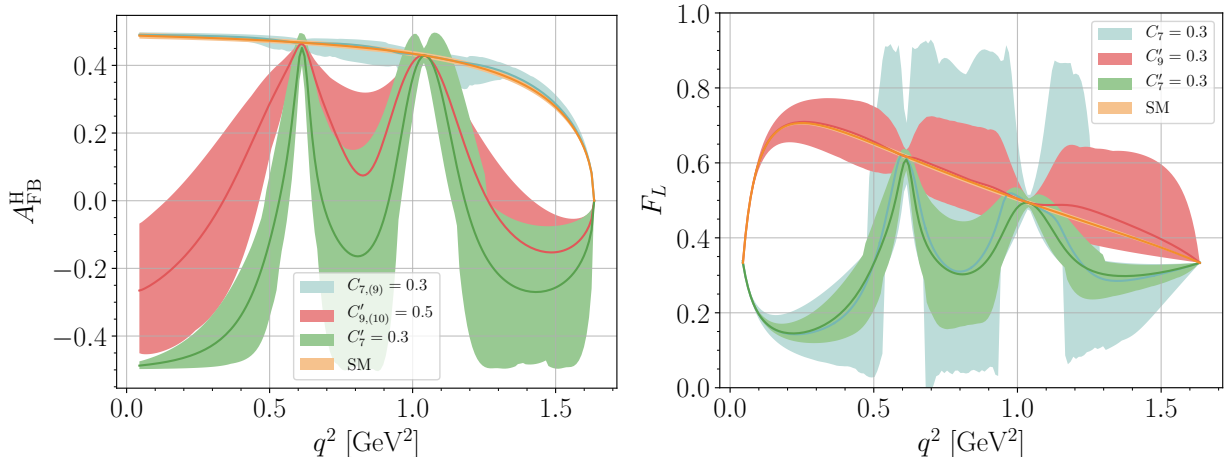


FIG. 1: The hadronic forward-backward asymmetry A_{FB}^{H} (14) (left plot) for $\Xi_c^+ \rightarrow \Sigma^+(\rightarrow p\pi^0)\mu^+\mu^-$ decays in the SM (orange) and in NP scenarios with C_7 or $C_9 = 0.3$, C'_9 or $C'_{10} = 0.5$ and $C'_7 = 0.3$ in blue, red and green, respectively. A NP scenario with C_{10} only is not shown, as it is indistinguishable from the SM. The right plot shows the fraction of longitudinally polarized dimuons F_L (10) in the SM (orange) and NP scenarios $C_7 = 0.3$, $C'_9 = 0.5$ and $C'_7 = 0.3$ in blue, red and green, respectively. Scenarios with C_9 and C'_{10} can not be distinguished from the SM with F_L and are not shown. The width of the bands stem predominantly from unknown strong phases.

(C_{10}), but strongly altered in scenarios involving right-handed currents C'_7 , C'_9 , C'_{10} , see the green and red bands in the left plot of Fig. 1.

The different impact of left-handed and right-handed NP contributions to A_{FB}^{H} can be attributed to the parity behavior of the angular observables. While K_{1ss} and K_{1cc} are P-even observables, K_{2ss} and K_{2cc} are P-odd. This leads to cancellations between numerator and denominator only in the case of left-handed contributions. To illustrate this consider A_{FB}^{H} for $m_\ell = 0$ in scenarios with C_9 and C'_{10} and all other NP coefficients switched off. It can be written as

$$A_{\text{FB}}^{\text{H}} = -\alpha \cdot \frac{\left(|C_9|^2 + |C_{10}|^2 - |C'_{10}|^2\right) A(q^2)\sqrt{s_+s_-}}{\left(\left(|C_9|^2 + |C_{10} - C'_{10}|^2\right) B(q^2)s_+ + \left(|C_9|^2 + |C_{10} + C'_{10}|^2\right) C(q^2)s_-\right)}, \quad (15)$$

where $A(q^2)$, $B(q^2)$ and $C(q^2)$ contain form factors and kinematics and are given in App. A, and $s_\pm = (m_{B_0} \pm m_{B_1})^2 - q^2$. For $C'_{10} = 0$ the coefficient C_9 cancels as in F_L , leading to the thin SM (orange) band. For $C_{10} \neq 0$ the same effect happens and $|C_9|^2 + |C_{10}|^2$ drops out. On the other hand, for $C'_{10} \neq 0$ the numerator is proportional to $|C_9|^2 - |C'_{10}|^2$, which does not cancel against the denominator and leads to NP deviations with q^2 -shape driven by $C_9^R(q^2)$. The same arguments holds for dipole couplings C_7 and $C_7^{(\prime)}$: A_{FB}^{H} is strongly sensitive to the latter, but not the former.

Note, interference terms between C_9 and C_7 softly break the exact cancellation (blue band around the SM). Again we stress that the requisite additional minus sign in front of the primed Wilson coefficients arises because K_{2ss} and K_{2cc} are P-odd.

B. $A_{\text{FB}}^{\ell\text{H}}$ and A_{FB}^{ℓ}

A third forward-backward asymmetry arises from combining leptonic and hadronic ones, $A_{\text{FB}}^{\ell\text{H}}$,

$$A_{\text{FB}}^{\ell\text{H}} = \frac{1}{d\Gamma/dq^2} \left[\int_0^1 - \int_{-1}^0 \right] \left[\int_0^1 - \int_{-1}^0 \right] \int_0^{2\pi} \frac{d^4\Gamma}{dq^2 d\cos\theta_\ell d\cos\theta_\pi} d\phi d\cos\theta_\ell d\cos\theta_\pi \quad (16)$$

$$= \frac{3}{4} \frac{K_{2c}}{2K_{1ss} + K_{1cc}}.$$

It is yet another charming null test of the SM, because C_{10} or C'_{10} are required to observe a non-vanishing signal.

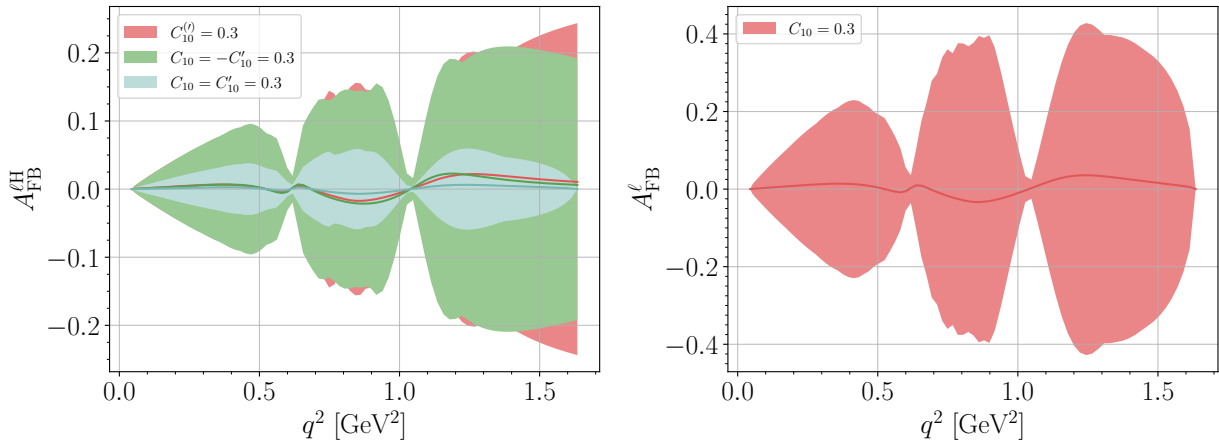


FIG. 2: The left plot shows the forward-backward asymmetry in both hadronic and leptonic scattering angles, $A_{\text{FB}}^{\ell\text{H}}$ (16) for $\Xi_c^+ \rightarrow \Sigma^+(\rightarrow p\pi^0)\mu^+\mu^-$ decays in NP scenarios with C_{10} or $C'_{10} = 0.3$, $C_{10} = -C'_{10} = 0.3$ and $C_{10} = C'_{10} = 0.3$ in red, green and blue, respectively. The right plot shows A_{FB}^{ℓ} (11) only in a $C_{10} = 0.3$ scenario. The width of the bands stem predominantly from unknown strong phases. Both $A_{\text{FB}}^{\ell\text{H}}$ and A_{FB}^{ℓ} are null tests of the SM (7).

In Fig. 2 $A_{\text{FB}}^{\ell\text{H}}$ is shown (left plot) for three different NP scenarios in red, green and blue for C_{10} or $C'_{10} = 0.3$, $C_{10} = -C'_{10} = 0.3$ and $C_{10} = C'_{10} = 0.3$, respectively. These benchmarks are chosen to illustrate the following: Firstly, C_{10} and C'_{10} contributions are indistinguishable within the large uncertainties induced by unknown strong phases entering in Eq. (3) and varied in the plot. Secondly, a scenario with $C_{10} = C'_{10}$ leads to a partial cancellation of contributions leading to a decreased signal with respect to $C_{10} = -C'_{10}$ scenarios. We also show A_{FB}^{ℓ} (11) in Fig. 2 (right plot)

for $C_{10} = 0.3$. We recall that A_{FB}^ℓ is a charm specific null test with sensitivity to the axial-vector coupling C_{10} down to the percent level. A_{FB}^ℓ vanishes at both, the low and the high q^2 endpoints.

The main benefit in studying $A_{\text{FB}}^{\ell\text{H}}$ in addition to A_{FB}^ℓ is complementarity. As pointed out in Ref. [12], A_{FB}^ℓ has sensitivity to C_{10} , but not necessarily C'_{10} , as this would require also NP contributions in C'_9 . In $A_{\text{FB}}^{\ell\text{H}}$ interference terms of type $C_9 C'_{10}$ exist, which are needed to observe a NP signal in a C'_{10} -only scenario. In addition, $A_{\text{FB}}^{\ell\text{H}}$ does not necessarily vanish at the high q^2 endpoint, and rather assumes a model-dependent value [35].

C. Model-independent analysis

To outline the strategy for disentangling NP contributions in charm baryon decays, we first summarize the sensitivities to single Wilson coefficients. The observables A_{FB}^ℓ and F_L appear in three-body decays, while A_{FB}^{H} and $A_{\text{FB}}^{\ell\text{H}}$ arise in self-analyzing four-body decays discussed in this work.

1. A_{FB}^ℓ is a null test that probes C_{10}
2. $A_{\text{FB}}^{\ell\text{H}}$ is a null test that probes C_{10} and C'_{10}
3. F_L probes C_7 and C'_7
4. A_{FB}^{H} probes C'_7 , C'_9 and C'_{10}

If there is no signal observed for the null tests A_{FB}^ℓ and $A_{\text{FB}}^{\ell\text{H}}$, one concludes that both C_{10} and C'_{10} are well below the percent level. In a next step F_L can be used to probe dipole contributions C_7 or C'_7 . To differentiate between the left-handed and right-handed dipole operators, A_{FB}^{H} can be employed. Similarly C'_9 can be extracted from A_{FB}^{H} , if F_L is SM-like. In a scenario with non-vanishing null tests, NP contributions to $C_{10}^{(\prime)}$ are evident. Here, again A_{FB}^{H} differentiates C_{10} and C'_{10} . In addition, A_{FB}^ℓ and $A_{\text{FB}}^{\ell\text{H}}$ reveal information on C'_{10} contributions. The only coefficient which can not be probed efficiently is C_9 , as it is dominated by the resonances C_9^R . As anticipated already in [12], a future simultaneous fit of Wilson coefficients and resonance parameters is then needed.

IV. FURTHER NULL TESTS

In this section we discuss further null test opportunities for rare charm baryon decays. We begin with the angular observables K_{3s} and K_{4s} (7) in Sec. IV A, discuss dineutrino modes in Sec. IV B

and present null tests that become available if the initial charm baryon is polarized (Sec. IV C). The study of charged lepton flavor violating modes offers even more clean null tests but is beyond the scope of this work.

A. K_{3s} and K_{4s}

The angular observables K_{3s} and K_{4s} vanish in the SM (7) or any SM extension with vanishing C_{10} and C'_{10} . Both K_{3s} and K_{4s} contain terms of the form $C_9 C_{10}$ and $C_9 C'_{10}$, just like $K_{2c} \propto A_{\text{FB}}^{\ell\text{H}}$, and unlike $K_{1c} \propto A_{\text{FB}}^{\ell}$. The latter requires additional NP coefficients to be sensitive to C'_{10} . This way, K_{3s} and K_{4s} are structurally similar to $A_{\text{FB}}^{\ell\text{H}}$, discussed in Sec. III B. All three of them probe C_{10} and C'_{10} , although with different combinations of form factors and NP coefficients.

At zero recoil, $K_{3s} = K_{1c} = 0$, and $K_{4s}(\text{d}\Gamma/\text{d}q^2)^{-1} = -K_{2c}(\text{d}\Gamma/\text{d}q^2)^{-1}$ and in general finite, with the value dependent on the model [35]. In Fig. 3 we show K_{3s} (right panel) and K_{4s} (left panel), normalized to the differential decay rate, for the same benchmarks with NP in $C_{10}^{(\prime)}$ as for $A_{\text{FB}}^{\ell\text{H}}$ in Fig. 2. While the different Wilson coefficient and form factor combinations of K_{3s} and K_{4s} only offer little qualitative complementarity compared to $A_{\text{FB}}^{\ell\text{H}}$, they do increase the statistics and enhance the sensitivity in a global analysis.

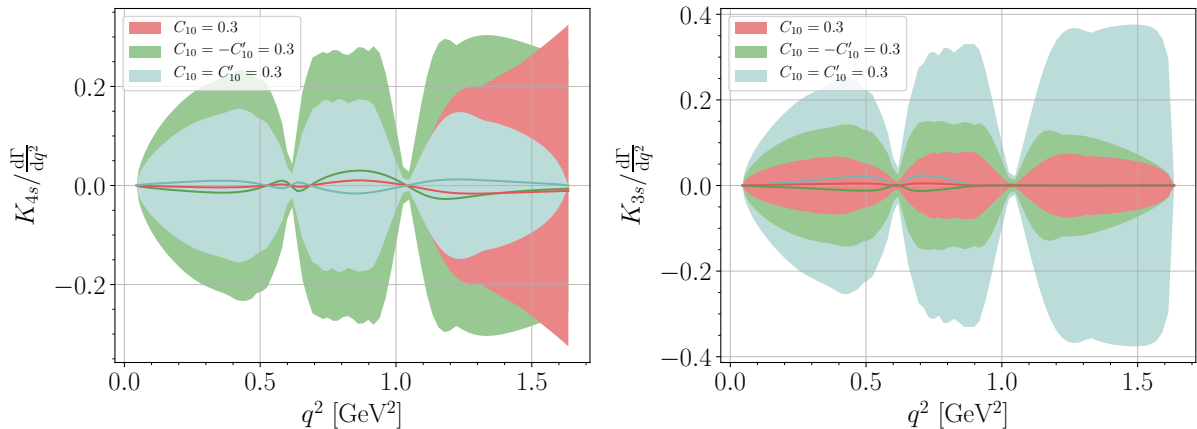


FIG. 3: The angular observables K_{4s} (left) and K_{3s} (right) normalized to the differential decay rate for $\Xi_c^+ \rightarrow \Sigma^+(\rightarrow p\pi^0)\mu^+\mu^-$ decays in different NP scenarios for C_{10} and C'_{10} . The width of the bands stem predominantly from unknown strong phases. Both observables are clean SM null tests (7).

B. Baryonic dineutrino modes

Dineutrino modes induced by $c \rightarrow u\nu\bar{\nu}$ transitions are severely GIM suppressed and negligible in the SM [1]. Any observation hence signals NP, making them prime candidates for searches [10]. The effective Hamiltonian reads

$$\mathcal{H}_{\text{eff}} = -\frac{4G_F}{\sqrt{2}} \sum_{ij} \left(C_L^{ij} Q_L^{ij} + C_R^{ij} Q_R^{ij} \right), \quad (17)$$

with $C_{L,R}^{ij}$ negligible in the SM and

$$Q_L^{ij} = (\bar{u}_L \gamma_\mu c_L)(\bar{\nu}_{Lj} \gamma^\mu \nu_{Li}), \quad Q_R^{ij} = (\bar{u}_R \gamma_\mu c_R)(\bar{\nu}_{Lj} \gamma^\mu \nu_{Li}). \quad (18)$$

Assuming the absence of light right-handed neutrinos, only these two operators exist for each combination of neutrino flavors i, j .

The self-analyzing four-body decays offer further opportunities for rare charm decays into dineutrinos. Specifically, this concerns the decays $\Xi_c^+ \rightarrow \Sigma^+ (\rightarrow p\pi^0)\nu\bar{\nu}$, $\Xi_c^0 \rightarrow \Lambda^0 (\rightarrow p\pi^-)\nu\bar{\nu}$, and $\Omega_c^0 \rightarrow \Xi^0 (\rightarrow \Lambda^0\pi^0)\nu\bar{\nu}$. The angular distribution is then given by

$$\frac{d^2\Gamma}{dq^2 d\cos\theta_\pi} = \int_{-1}^1 \int_0^{2\pi} \frac{d^4\Gamma}{dq^2 d\cos\theta_\pi d\cos\theta_\ell d\phi} d\phi d\cos\theta_\ell = 2K_{1ss} + K_{1cc} + (2K_{2ss} + K_{2cc}) \cos\theta_\pi, \quad (19)$$

and accessible without reconstructing the neutrinos [35]. Note, here, in K_{1ss} , K_{1cc} , K_{2ss} and K_{2cc} one has to replace $C_9 = -C_{10} = \frac{4\pi}{\alpha_e} C_L^{ij}/2$ and $C'_9 = -C'_{10} = \frac{4\pi}{\alpha_e} C_R^{ij}/2$, skip the m_ℓ^2 terms and incoherently sum the neutrino flavors ij . This gives rise to two independent observables, the differential decay rate and the hadronic forward-backward asymmetry A_{FB}^{H} (14).

The hadronic forward-backward asymmetry A_{FB}^{H} is obtained by integrating over the leptons phase space, and therefore can be measured in dineutrino modes. It reads

$$A_{\text{FB}}^{\text{H}}(B_0 \rightarrow B_1(\rightarrow B_2\pi)\nu\bar{\nu}) = -\alpha \cdot \frac{(|C_L|^2 - |C_R|^2) A(q^2) \sqrt{s_+ s_-}}{|C_L - C_R|^2 B(q^2)_{s_+} + |C_L + C_R|^2 C(q^2)_{s_-}} \quad (20)$$

and probes C_R/C_L . To ease notation here we omit the flavor indices. In the limit $C_R = 0$, the asymmetry becomes free of Wilson coefficients,

$$A_{\text{FB}}^{\text{H}}(B_0 \rightarrow B_1(\rightarrow B_2\pi)\nu\bar{\nu}) = -\alpha \cdot \frac{A(q^2) \sqrt{s_+ s_-}}{B(q^2)_{s_+} + C(q^2)_{s_-}}. \quad (21)$$

The functions $A(q^2)$, $B(q^2)$ and $C(q^2)$ contain form factors and kinematics and can be seen in App. A.

Upper limits on the branching ratios can be derived from a global EFT-analysis [10]

$$\begin{aligned}
\mathcal{B}(\Xi_c^+ \rightarrow \Sigma^+(\rightarrow p\pi^0)\nu\bar{\nu}) &\lesssim 3.9 \times 10^{-5}, \\
\mathcal{B}(\Xi_c^0 \rightarrow \Lambda^0(\rightarrow p\pi^-)\nu\bar{\nu}) &\lesssim 3.6 \times 10^{-6}, \\
\mathcal{B}(\Omega_c^0 \rightarrow \Xi^0(\rightarrow \Lambda^0\pi^0)\nu\bar{\nu}) &\lesssim 7.1 \times 10^{-5},
\end{aligned}
\tag{22}$$

in agreement with results in Ref. [12]. The upper limits are stronger when assumptions on the lepton flavor are made [10]. These are given in the next equation, with the first entry corresponding to charged lepton flavor conservation, and the even stronger one in parentheses assuming lepton universality:

$$\begin{aligned}
\mathcal{B}(\Xi_c^+ \rightarrow \Sigma^+(\rightarrow p\pi^0)\nu\bar{\nu}) &\lesssim 1.1 \times 10^{-5}, \quad (1.9 \times 10^{-6}), \\
\mathcal{B}(\Xi_c^0 \rightarrow \Lambda^0(\rightarrow p\pi^-)\nu\bar{\nu}) &\lesssim 1.0 \times 10^{-6}, \quad (1.7 \times 10^{-7}), \\
\mathcal{B}(\Omega_c^0 \rightarrow \Xi^0(\rightarrow \Lambda^0\pi^0)\nu\bar{\nu}) &\lesssim 1.9 \times 10^{-5}, \quad (3.4 \times 10^{-6}).
\end{aligned}
\tag{23}$$

C. Polarized Charm baryons

Let us point out that studying decays of polarized charmed baryons introduces further null test observables on top of those in (7). We identify in total eight additional angular null tests probing leptonic axial vector currents, *i.e.*, $C_{10}^{(\prime)}$ [6], which are proportional to the initial B_0 -polarization P_{B_0} ,

$$K_{13}, K_{16}, K_{18}, K_{20}, K_{22}, K_{24}, K_{26}, K_{28}|_{\text{SM}} \simeq 0, \tag{24}$$

with the differential distribution [34] given in App. C. Among these, K_{13} , K_{22} and K_{24} do not vanish for $\alpha = 0$ and hence can be studied in the simpler three-body decays, including $\Lambda_c \rightarrow p\mu^+\mu^-$. We note that $K_{13} = -P_{B_0}K_{2c}$, anticipating that a study with polarized baryons can access some of the null tests, here $A_{\text{FB}}^{\ell\text{H}}$, that otherwise require a self-analyzing four-body decay. If in the future high luminosity sources of polarized Λ_c 's or other charmed baryons can be used, see [36] for LHC and e^+e^- -collider possibilities, we would like to come back to explore these observables and their NP reach in charm in more detail.

V. CONCLUSIONS

We perform a full angular analysis of baryonic $|\Delta c| = |\Delta u| = 1$ four-body decays with self-analyzing secondary baryon to explore the BSM reach. We identify several such modes:

$\Xi_c^+ \rightarrow \Sigma^+ (\rightarrow p\pi^0)\ell^+\ell^-$, $\Xi_c^0 \rightarrow \Lambda^0 (\rightarrow p\pi^-)\ell^+\ell^-$ and $\Omega_c^0 \rightarrow \Xi^0 (\rightarrow \Lambda^0\pi^0)\ell^+\ell^-$, with sizable decay parameter, see Table I. The full differential distribution of an unpolarized initial charm baryon (5) features ten angular observables, seven more, and with different NP sensitivities, than the ones available with three-body decays such as $\Lambda_c \rightarrow p\ell^+\ell^-$. We point out three new, clean null tests of the SM, K_{2c} , K_{3s} and K_{4s} (7). Just like the leptonic forward-backward asymmetry $A_{\text{FB}}^\ell \propto K_{1c}$ (11), their SM contribution can be safely neglected because the GIM-mechanism switches off axial-vector couplings of the leptons, a feature previously exploited also for the $D \rightarrow \pi\pi\ell^+\ell^-$ angular distribution [6]. We also find that the hadronic forward-backward asymmetry A_{FB}^{H} (14), although not a null test, can cleanly signal BSM physics in right-handed currents, $C'_{7,9,10}$, illustrated in Fig. 1.

The angular observables in four-body decays enable highly diagnostic tests of BSM couplings. Concrete analysis of the NP sensitivity, see Section III, shows that already four observables, the longitudinal polarization fraction F_L (10), together with the forward-backward asymmetries A_{FB}^{H} , A_{FB}^ℓ and $A_{\text{FB}}^{\ell\text{H}}$ (16) allow to pin down BSM Wilson coefficients in one go:

If there is sizable NP only in F_L , it is C_7 .

If there is sizable NP only in F_L and A_{FB}^{H} , it is C'_7 .

If there is sizable NP only in A_{FB}^{H} , it is C'_9 .

If there is sizable NP only in $A_{\text{FB}}^{\ell\text{H}}$ and A_{FB}^{H} , it is C'_{10} .

If there is sizable NP only in A_{FB}^ℓ and $A_{\text{FB}}^{\ell\text{H}}$, it is C_{10} .

The price to pay for the self-analyzing (quasi) four-body decay is the limitation to specific charm baryon modes; the suppression from the secondary baryon decays is modest since branching ratios are at least 50 %. Experimental analysis is suitable for (advanced stages of) high luminosity flavor factories LHCb [21], Belle II [22], BES III [23], and possible future machines [24, 25].

Decays of polarized charmed baryon offer further GIM-based null tests (24), some of which persist in the simpler three-body decays. Their exploration should be pursued further if in the future high luminosity sources of polarized Λ_c 's or other charmed baryons become available.

We note in passing that the hadronic forward-backward asymmetry is obtained by integrating over the leptons phase space, and therefore can be measured in dineutrino modes $\Xi_c^+ \rightarrow \Sigma^+ (\rightarrow p\pi^0)\nu\bar{\nu}$, $\Xi_c^0 \rightarrow \Lambda^0 (\rightarrow p\pi^-)\nu\bar{\nu}$ and $\Omega_c^0 \rightarrow \Xi^0 (\rightarrow \Lambda^0\pi^0)\nu\bar{\nu}$, briefly discussed in Sec. IV B, too.

We conclude that rare decays of charm baryons contribute extensively to our endeavor to search for NP. Dedicated computations of form factors for $\Xi_c^+ \rightarrow \Sigma^+$, $\Xi_c^0 \rightarrow \Lambda^0$ and $\Omega_c^0 \rightarrow \Xi^0$ transitions are desirable. As anticipated in [12], a simultaneous fit of $|\Delta c| = |\Delta u| = 1$ Wilson coefficients and resonance parameters is called for. The sensitivity of such a fit is enriched by the new presented observables in four-body baryon decays.

Acknowledgments

We are happy to thank Dominik Mittel for useful discussions. This work is supported by the *Studienstiftung des Deutschen Volkes* (MG) and in part by the *Bundesministerium für Bildung und Forschung* (BMBF) under project number 05H21PECL2 (GH).

Appendix A: Helicity Amplitudes

Following [14] we introduce the contributions to the angular observables (6)

$$\begin{aligned}
S^{mm'} &= N^2 \cdot \text{Re} \left[\mathcal{H}_{\frac{1}{2},t}^m \mathcal{H}_{\frac{1}{2},t}^{\dagger m'} + \mathcal{H}_{-\frac{1}{2},t}^m \mathcal{H}_{-\frac{1}{2},t}^{\dagger m'} \right], \\
S_P^{mm'} &= N^2 \cdot \text{Re} \left[\mathcal{H}_{\frac{1}{2},t}^m \mathcal{H}_{\frac{1}{2},t}^{\dagger m'} - \mathcal{H}_{-\frac{1}{2},t}^m \mathcal{H}_{-\frac{1}{2},t}^{\dagger m'} \right], \\
U^{mm'} &= N^2 \cdot \text{Re} \left[\mathcal{H}_{\frac{1}{2},1}^m \mathcal{H}_{\frac{1}{2},1}^{\dagger m'} + \mathcal{H}_{-\frac{1}{2},-1}^m \mathcal{H}_{-\frac{1}{2},-1}^{\dagger m'} \right], \\
P^{mm'} &= N^2 \cdot \text{Re} \left[\mathcal{H}_{\frac{1}{2},1}^m \mathcal{H}_{\frac{1}{2},1}^{\dagger m'} - \mathcal{H}_{-\frac{1}{2},-1}^m \mathcal{H}_{-\frac{1}{2},-1}^{\dagger m'} \right], \\
L^{mm'} &= N^2 \cdot \text{Re} \left[\mathcal{H}_{\frac{1}{2},0}^m \mathcal{H}_{\frac{1}{2},0}^{\dagger m'} + \mathcal{H}_{-\frac{1}{2},0}^m \mathcal{H}_{-\frac{1}{2},0}^{\dagger m'} \right], \\
L_P^{mm'} &= N^2 \cdot \text{Re} \left[\mathcal{H}_{\frac{1}{2},0}^m \mathcal{H}_{\frac{1}{2},0}^{\dagger m'} - \mathcal{H}_{-\frac{1}{2},0}^m \mathcal{H}_{-\frac{1}{2},0}^{\dagger m'} \right], \\
I_{1P}^{mm'} &= \frac{N^2}{4} \text{Re} \left[\mathcal{H}_{\frac{1}{2},1}^m \mathcal{H}_{-\frac{1}{2},0}^{\dagger m'} + \mathcal{H}_{-\frac{1}{2},0}^m \mathcal{H}_{\frac{1}{2},1}^{\dagger m'} - \mathcal{H}_{\frac{1}{2},0}^m \mathcal{H}_{-\frac{1}{2},-1}^{\dagger m'} - \mathcal{H}_{-\frac{1}{2},-1}^m \mathcal{H}_{\frac{1}{2},0}^{\dagger m'} \right], \\
I_2^{mm'} &= \frac{N^2}{4} \text{Im} \left[\mathcal{H}_{\frac{1}{2},1}^m \mathcal{H}_{-\frac{1}{2},0}^{\dagger m'} - \mathcal{H}_{-\frac{1}{2},0}^m \mathcal{H}_{\frac{1}{2},1}^{\dagger m'} - \mathcal{H}_{\frac{1}{2},0}^m \mathcal{H}_{-\frac{1}{2},-1}^{\dagger m'} + \mathcal{H}_{-\frac{1}{2},-1}^m \mathcal{H}_{\frac{1}{2},0}^{\dagger m'} \right], \\
I_3^{mm'} &= \frac{N^2}{4} \text{Re} \left[\mathcal{H}_{\frac{1}{2},1}^m \mathcal{H}_{-\frac{1}{2},0}^{\dagger m'} + \mathcal{H}_{-\frac{1}{2},0}^m \mathcal{H}_{\frac{1}{2},1}^{\dagger m'} + \mathcal{H}_{\frac{1}{2},0}^m \mathcal{H}_{-\frac{1}{2},-1}^{\dagger m'} + \mathcal{H}_{-\frac{1}{2},-1}^m \mathcal{H}_{\frac{1}{2},0}^{\dagger m'} \right], \\
I_{4P}^{mm'} &= \frac{N^2}{4} \text{Im} \left[\mathcal{H}_{\frac{1}{2},1}^m \mathcal{H}_{-\frac{1}{2},0}^{\dagger m'} - \mathcal{H}_{-\frac{1}{2},0}^m \mathcal{H}_{\frac{1}{2},1}^{\dagger m'} + \mathcal{H}_{\frac{1}{2},0}^m \mathcal{H}_{-\frac{1}{2},-1}^{\dagger m'} - \mathcal{H}_{-\frac{1}{2},-1}^m \mathcal{H}_{\frac{1}{2},0}^{\dagger m'} \right],
\end{aligned} \tag{A1}$$

in terms of helicity amplitudes $\mathcal{H}_{\lambda_\Sigma, \lambda_\gamma}^m$, where λ_Σ and λ_γ denote the helicities of the Σ baryon and the effective current $\gamma^*(\rightarrow \ell\ell)$, respectively. λ_Σ can therefore assume values of $\pm\frac{1}{2}$, whereas λ_γ takes values of $0, \pm 1$, and we further distinguish $\lambda_\gamma = t$ in the $J_\gamma = 0$ case and $\lambda_\gamma = 0$ in the $J_\gamma = 1$ case. The superscript $m^{(\prime)}$ distinguishes between leptonic vector ($m^{(\prime)} = 1$) and axial-vector ($m^{(\prime)} = 2$) contributions. While the former receive contributions from $C_7^{(\prime)}$ and $C_9^{(\prime)}$, the latter are induced by $C_{10}^{(\prime)}$, hence vanish in the SM. The helicity amplitudes $\mathcal{H}_{\lambda_\Sigma, \lambda_\gamma}^m$ are obtained by summing the contributions from individual hadronic matrix elements, $\mathcal{H}_{\lambda_\Sigma, \lambda_\gamma}^{a,m}$, hence $\mathcal{H}_{\lambda_\Sigma, \lambda_\gamma}^m = \sum_a \mathcal{H}_{\lambda_\Sigma, \lambda_\gamma}^{a,m}$. Here, $a = 1, 2$ correspond to dipole contributions from $C_7^{(\prime)}$ and $a = 3, 4$ to those from 4-fermion operators $C_9^{(\prime)}$ and $C_{10}^{(\prime)}$. Contributions $a = 1$ and $a = 3$ are induced by quark-level vector currents,

hence proportional to $C + C'$, whereas contributions $a = 2$ and $a = 4$ are induced by quark-level axial-vector currents, hence $\propto C - C'$. Due to parity, flipping the helicities results in a minus sign for the amplitudes $a = 2$ and $a = 4$. The amplitudes $\mathcal{H}_{\lambda_\Sigma, \lambda_\gamma}^{1,2}$ are then decomposed as

$$\begin{aligned}
\mathcal{H}_{\lambda_\Sigma, \lambda_\gamma}^1 &= \mathcal{H}_{\lambda_\Sigma, \lambda_\gamma}^{1,1} + \mathcal{H}_{\lambda_\Sigma, \lambda_\gamma}^{2,1} + \mathcal{H}_{\lambda_\Sigma, \lambda_\gamma}^{3,1} + \mathcal{H}_{\lambda_\Sigma, \lambda_\gamma}^{4,1}, \\
\mathcal{H}_{-\lambda_\Sigma, -\lambda_\gamma}^1 &= \mathcal{H}_{\lambda_\Sigma, \lambda_\gamma}^{1,1} - \mathcal{H}_{\lambda_\Sigma, \lambda_\gamma}^{2,1} + \mathcal{H}_{\lambda_\Sigma, \lambda_\gamma}^{3,1} - \mathcal{H}_{\lambda_\Sigma, \lambda_\gamma}^{4,1}, \\
\mathcal{H}_{\lambda_\Sigma, \lambda_\gamma}^2 &= \mathcal{H}_{\lambda_\Sigma, \lambda_\gamma}^{3,2} + \mathcal{H}_{\lambda_\Sigma, \lambda_\gamma}^{4,2}, \\
\mathcal{H}_{-\lambda_\Sigma, -\lambda_\gamma}^2 &= \mathcal{H}_{\lambda_\Sigma, \lambda_\gamma}^{3,2} - \mathcal{H}_{\lambda_\Sigma, \lambda_\gamma}^{4,2}.
\end{aligned} \tag{A2}$$

For convenience we give in the following a list of single contributions but stress that except for the different decay modes these equations are equivalent to Eqs. (C3)-(C5) of Ref. [12]. The helicity of the initial, charm baryon satisfies $\lambda_{\Xi_c} = -\lambda_\Sigma + \lambda_\gamma$.

$$\lambda_{\Xi_c} = \frac{1}{2}, \lambda_\gamma = t:$$

$$\begin{aligned}
\mathcal{H}_{-\frac{1}{2}, t}^{1,1} &= 0, \\
\mathcal{H}_{-\frac{1}{2}, t}^{2,1} &= 0, \\
\mathcal{H}_{-\frac{1}{2}, t}^{3,1(2)} &= (C_{9(10)} + C'_{9(10)}) \frac{\sqrt{s_+}}{\sqrt{q^2}} f_0(q^2) (m_{\Xi_c} - m_\Sigma), \\
\mathcal{H}_{-\frac{1}{2}, t}^{4,1(2)} &= (C_{9(10)} - C'_{9(10)}) \frac{\sqrt{s_-}}{\sqrt{q^2}} g_0(q^2) (m_{\Xi_c} + m_\Sigma),
\end{aligned} \tag{A3}$$

$$\lambda_{\Xi_c} = -\frac{1}{2}, \lambda_\gamma = 0:$$

$$\begin{aligned}
\mathcal{H}_{\frac{1}{2}, 0}^{1,1} &= (C_7 + C'_7) \frac{2m_c}{\sqrt{q^2}} \sqrt{s_-} h_+(q^2), \\
\mathcal{H}_{\frac{1}{2}, 0}^{2,1} &= -(C_7 - C'_7) \frac{2m_c}{\sqrt{q^2}} \sqrt{s_+} \tilde{h}_+(q^2), \\
\mathcal{H}_{\frac{1}{2}, 0}^{3,1(2)} &= (C_{9(10)} + C'_{9(10)}) \frac{1}{\sqrt{q^2}} \sqrt{s_-} f_+(q^2) (m_{\Xi_c} + m_\Sigma), \\
\mathcal{H}_{\frac{1}{2}, 0}^{4,1(2)} &= -(C_{9(10)} - C'_{9(10)}) \frac{1}{\sqrt{q^2}} \sqrt{s_+} g_+(q^2) (m_{\Xi_c} - m_\Sigma),
\end{aligned} \tag{A4}$$

$$\lambda_{\Xi_c} = \frac{1}{2}, \lambda_\gamma = 1:$$

$$\begin{aligned}
\mathcal{H}_{\frac{1}{2}, 1}^{1,1} &= \sqrt{2} (C_7 + C'_7) \frac{2m_c}{q^2} \sqrt{s_-} h_\perp(q^2) (m_{\Xi_c} + m_\Sigma), \\
\mathcal{H}_{\frac{1}{2}, 1}^{2,1} &= -\sqrt{2} (C_7 - C'_7) \frac{2m_c}{q^2} \sqrt{s_+} \tilde{h}_\perp(q^2) (m_{\Xi_c} - m_\Sigma), \\
\mathcal{H}_{\frac{1}{2}, 1}^{3,1(2)} &= \sqrt{2} (C_{9(10)} + C'_{9(10)}) \sqrt{s_-} f_\perp(q^2), \\
\mathcal{H}_{\frac{1}{2}, 1}^{4,1(2)} &= -\sqrt{2} (C_{9(10)} - C'_{9(10)}) \sqrt{s_+} g_\perp(q^2).
\end{aligned} \tag{A5}$$

Using the helicity amplitudes we obtain for the contributions in Eq. (A1)

$$\begin{aligned}
U^{11} &= 4N^2 \cdot \left[\left| (C_7 + C'_7) \frac{2m_c}{q^2} (m_{\Xi_c^+} + m_{\Sigma^+}) h_{\perp} + (C_9 + C'_9) f_{\perp} \right|^2 \cdot s_{-} \right. \\
&\quad \left. + \left| (C_7 - C'_7) \frac{2m_c}{q^2} (m_{\Xi_c^+} - m_{\Sigma^+}) \tilde{h}_{\perp} + (C_9 - C'_9) g_{\perp} \right|^2 \cdot s_{+} \right], \\
L^{11} &= \frac{2N^2}{q^2} \cdot \left[\left| (C_7 + C'_7) 2m_c h_{+} + (C_9 + C'_9) (m_{\Xi_c^+} + m_{\Sigma^+}) f_{+} \right|^2 \cdot s_{-} \right. \\
&\quad \left. + \left| (C_7 - C'_7) 2m_c \tilde{h}_{+} + (C_9 - C'_9) (m_{\Xi_c^+} - m_{\Sigma^+}) g_{+} \right|^2 \cdot s_{+} \right], \\
U^{22} &= 4N^2 \cdot \left[\left| (C_{10} + C'_{10}) f_{\perp} \right|^2 \cdot s_{-} + \left| (C_{10} - C'_{10}) g_{\perp} \right|^2 \cdot s_{+} \right], \\
L^{22} &= \frac{2N^2}{q^2} \cdot \left[\left| (C_{10} + C'_{10}) (m_{\Xi_c^+} + m_{\Sigma^+}) f_{+} \right|^2 \cdot s_{-} + \left| (C_{10} - C'_{10}) (m_{\Xi_c^+} - m_{\Sigma^+}) g_{+} \right|^2 \cdot s_{+} \right], \\
S^{22} &= \frac{2N^2}{q^2} \cdot \left[\left| (C_{10} + C'_{10}) (m_{\Xi_c^+} - m_{\Sigma^+}) f_0 \right|^2 \cdot s_{+} + \left| (C_{10} - C'_{10}) (m_{\Xi_c^+} + m_{\Sigma^+}) g_0 \right|^2 \cdot s_{-} \right], \\
P^{12} &= -8N^2 \cdot \left[\text{Re}((C_7 - C'_7) (C_{10}^* + C'_{10}{}^*)) \frac{m_c}{q^2} (m_{\Xi_c^+} - m_{\Sigma^+}) f_{\perp} \tilde{h}_{\perp} \right. \\
&\quad + \text{Re}((C_7 + C'_7) (C_{10}^* - C'_{10}{}^*)) \frac{m_c}{q^2} (m_{\Xi_c^+} + m_{\Sigma^+}) g_{\perp} h_{\perp} \\
&\quad \left. + \text{Re}(C_9 C_{10}^* - C'_9 C'_{10}{}^*) g_{\perp} f_{\perp} \right] \cdot \sqrt{s_{+} s_{-}}.
\end{aligned} \tag{A6}$$

Here, $N^2 = \frac{G_F^2 \alpha_c^2 v \sqrt{\lambda(m_{\Xi_c^+}^2, m_{\Sigma^+}^2, q^2)}}{3 \cdot 2^{11} \pi^5 m_{\Xi_c^+}^3}$ with the Källén function $\lambda(a, b, c) = a^2 + b^2 + c^2 - 2(ab + ac + bc)$ and $s_{\pm} = (m_{\Xi_c^+} \pm m_{\Sigma^+})^2 - q^2$. The contributions in Eq. (A6) are those relevant to three-body decays and have already been given in Ref. [12]. The additional contributions that arise in the full, four-

body angular distribution (5) read

$$\begin{aligned}
L_P^{11} &= -\frac{4N^2}{q^2} \cdot \text{Re} \left[\left((C_7 + C'_7) 2m_c h_+ + (C_9 + C'_9) (m_{\Xi_c^+} + m_{\Sigma^+}) f_+ \right) \right. \\
&\quad \left. \cdot \left((C_7^* - C_7'^*) 2m_c \tilde{h}_+ + (C_9^* - C_9'^*) (m_{\Xi_c^+} - m_{\Sigma^+}) g_+ \right) \right] \cdot \sqrt{s_+ s_-}, \\
P^{11} &= -8N^2 \cdot \text{Re} \left[\left((C_7 + C'_7) \frac{2m_c}{q^2} h_\perp (m_{\Xi_c^+} + m_{\Sigma^+}) + (C_9 + C'_9) f_\perp \right) \right. \\
&\quad \left. \cdot \left((C_7^* - C_7'^*) \frac{2m_c}{q^2} \tilde{h}_\perp (m_{\Xi_c^+} - m_{\Sigma^+}) + (C_9^* - C_9'^*) g_\perp \right) \right] \cdot \sqrt{s_+ s_-}, \\
L_P^{22} &= -\frac{4N^2}{q^2} \cdot \left[(|C_{10}|^2 - |C'_{10}|^2) f_+ g_+ (m_{\Xi_c^+}^2 - m_{\Sigma^+}^2) \right] \cdot \sqrt{s_+ s_-}, \\
P^{22} &= -8N^2 \cdot \left[(|C_{10}|^2 - |C'_{10}|^2) f_\perp g_\perp \right] \cdot \sqrt{s_+ s_-}, \\
U^{12} &= 4N^2 \cdot \left[\left(\text{Re}((C_7 + C'_7)(C_{10}^* + C_{10}'^*)) f_\perp h_\perp \frac{2m_c}{q^2} (m_{\Xi_c^+} + m_{\Sigma^+}) \right. \right. \\
&\quad \left. \left. + \text{Re}((C_9 + C'_9)(C_{10}^* + C_{10}'^*)) f_\perp^2 \right) \cdot s_- \right. \\
&\quad \left. + \left(\text{Re}((C_7 - C'_7)(C_{10}^* - C_{10}'^*)) g_\perp \tilde{h}_\perp \frac{2m_c}{q^2} (m_{\Xi_c^+} - m_{\Sigma^+}) \right. \right. \\
&\quad \left. \left. + \text{Re}((C_9 - C'_9)(C_{10}^* - C_{10}'^*)) g_\perp^2 \right) \cdot s_+ \right], \\
S_P^{22} &= -\frac{4N^2}{q^2} \cdot \left[(|C_{10}|^2 - |C'_{10}|^2) f_0 g_0 (m_{\Xi_c^+}^2 - m_{\Sigma^+}^2) \right] \cdot \sqrt{s_+ s_-}.
\end{aligned} \tag{A7}$$

The interference terms are given by

$$\begin{aligned}
I_{1P}^{11} &= N^2 \sqrt{\frac{2}{q^2}} \cdot \left[\text{Re}((C_7 - C'_7)(C_7^* + C'^*_7)) \frac{4m_c^2}{q^2} \cdot (\tilde{h}_+ h_\perp (m_{\Xi_c^+} + m_{\Sigma^+}) - h_+ \tilde{h}_\perp (m_{\Xi_c^+} - m_{\Sigma^+})) \right. \\
&\quad + \text{Re}((C_9 - C'_9)(C_9^* + C'^*_9)) \cdot (g_+ f_\perp (m_{\Xi_c^+} - m_{\Sigma^+}) - f_+ g_\perp (m_{\Xi_c^+} + m_{\Sigma^+})) \\
&\quad + \text{Re}((C_9 - C'_9)(C_7^* + C'^*_7)) 2m_c \cdot \left(g_+ h_\perp \frac{m_{\Xi_c^+}^2 - m_{\Sigma^+}^2}{q^2} - h_+ g_\perp \right) \\
&\quad \left. + \text{Re}((C_7 - C'_7)(C_9^* + C'^*_9)) 2m_c \cdot \left(\tilde{h}_+ f_\perp - f_+ \tilde{h}_\perp \frac{m_{\Xi_c^+}^2 - m_{\Sigma^+}^2}{q^2} \right) \right] \cdot \sqrt{s_+ s_-}, \\
I_{1P}^{22} &= N^2 \sqrt{\frac{2}{q^2}} \cdot \left[(|C_{10}|^2 - |C'_{10}|^2) \cdot (f_\perp g_+ (m_{\Xi_c^+} - m_{\Sigma^+}) - f_+ g_\perp (m_{\Xi_c^+} + m_{\Sigma^+})) \right] \cdot \sqrt{s_+ s_-}, \\
I_2^{11} &= 2m_c N^2 \sqrt{\frac{2}{q^2}} \cdot \left[\text{Im}((C_9 + C'_9)(C_7^* + C'^*_7)) \cdot \left(f_\perp h_+ - f_+ h_\perp \frac{(m_{\Xi_c^+} + m_{\Sigma^+})^2}{q^2} \right) \cdot s_- \right. \\
&\quad \left. - \text{Im}((C_9 - C'_9)(C_7^* - C'^*_7)) \cdot \left(g_\perp \tilde{h}_+ - g_+ \tilde{h}_\perp \frac{(m_{\Xi_c^+} - m_{\Sigma^+})^2}{q^2} \right) \cdot s_+ \right], \\
I_2^{22} &= 0, \\
I_3^{12} &= N^2 \sqrt{\frac{2}{q^2}} \cdot \left[\text{Re}((C_7 + C'_7)(C_{10}^* + C'_{10}{}^*)) m_c \cdot \left(h_+ f_\perp + f_+ h_\perp \frac{(m_{\Xi_c^+} + m_{\Sigma^+})^2}{q^2} \right) \cdot s_- \right. \\
&\quad - \text{Re}((C_7 - C'_7)(C_{10}^* - C'_{10}{}^*)) m_c \cdot \left(\tilde{h}_+ g_\perp + g_+ \tilde{h}_\perp \frac{(m_{\Xi_c^+} - m_{\Sigma^+})^2}{q^2} \right) \cdot s_+ \\
&\quad + \text{Re}((C_9 + C'_9)(C_{10}^* + C'_{10}{}^*)) \cdot (f_+ f_\perp (m_{\Xi_c^+} + m_{\Sigma^+})) \cdot s_- \\
&\quad \left. - \text{Re}((C_9 - C'_9)(C_{10}^* - C'_{10}{}^*)) \cdot (g_+ g_\perp (m_{\Xi_c^+} - m_{\Sigma^+})) \cdot s_+ \right], \\
I_{4P}^{12} &= N^2 \sqrt{\frac{2}{q^2}} \cdot \left[\text{Im}((C_7 + C'_7)(C_{10}^* - C'_{10}{}^*)) m_c \cdot \left(h_\perp g_+ \frac{m_{\Xi_c^+}^2 - m_{\Sigma^+}^2}{q^2} + h_+ g_\perp \right) \right. \\
&\quad + \text{Im}((C_7 - C'_7)(C_{10}^* + C'_{10}{}^*)) m_c \cdot \left(\tilde{h}_\perp f_+ \frac{m_{\Xi_c^+}^2 - m_{\Sigma^+}^2}{q^2} + \tilde{h}_+ f_\perp \right) \\
&\quad + \text{Im}((C_9 + C'_9)(C_{10}^* - C'_{10}{}^*)) \frac{1}{2} \cdot (f_\perp g_+ (m_{\Xi_c^+} - m_{\Sigma^+}) + f_+ g_\perp (m_{\Xi_c^+} + m_{\Sigma^+})) \\
&\quad \left. + \text{Im}((C_9 - C'_9)(C_{10}^* + C'_{10}{}^*)) \frac{1}{2} \cdot (g_\perp f_+ (m_{\Xi_c^+} + m_{\Sigma^+}) + g_+ f_\perp (m_{\Xi_c^+} - m_{\Sigma^+})) \right] \\
&\quad \cdot \sqrt{s_+ s_-}.
\end{aligned} \tag{A8}$$

All additional contributions (A7), (A8) except U^{12} , I_2^{11} and I_3^{12} are P-odd, that is, change sign for $C_i \leftrightarrow C'_i$, and vanish for $C_i = C'_i$.

In Eqs. (15), (20) and (21) the following q^2 -dependent functions appear

$$\begin{aligned} A(q^2) &= 2f_{\perp}g_{\perp} + f_{+}g_{+} \frac{m_{B_0}^2 - m_{B_1}^2}{q^2}, \\ B(q^2) &= 2g_{\perp}^2 + g_{+}^2 \frac{(m_{B_0} - m_{B_1})^2}{q^2}, \\ C(q^2) &= 2f_{\perp}^2 + f_{+}^2 \frac{(m_{B_0} + m_{B_1})^2}{q^2}. \end{aligned} \quad (\text{A9})$$

Appendix B: Helicity amplitude description of $B_1 \rightarrow B_2\pi$

The secondary baryonic decay $B_1 \rightarrow B_2\pi$, here discussed for $\Sigma^+ \rightarrow p\pi^0$, can be parameterized by the sum, α_+ , and the difference, α_- , of the helicity amplitudes $h_{\lambda_p}^{\Sigma}(\lambda_{\Sigma})$ squared

$$\alpha_{\pm} = \left| h_{\frac{1}{2}}^{\Sigma} \left(\lambda_{\Sigma} = \frac{1}{2} \right) \right|^2 \pm \left| h_{-\frac{1}{2}}^{\Sigma} \left(\lambda_{\Sigma} = -\frac{1}{2} \right) \right|^2. \quad (\text{B1})$$

The helicity amplitudes of non-leptonic baryon decays involving a spin-0 meson, here taken to be a pion, can be parametrized as

$$h_{\lambda_p}^{\Sigma}(\lambda_{\Sigma}) = G_F m_{\pi}^2 \bar{u}_p(\lambda_p)(A - B\gamma_5)u_{\Sigma}(\lambda_{\Sigma}), \quad (\text{B2})$$

where A and B are complex constants [37] and m_{π} the pion mass. We compute the amplitude in the rest frame of the Σ^+ with the z -axis pointing in the direction of the proton momentum. The spinors then take the form

$$\begin{aligned} u_{\Sigma} \left(p, \lambda_{\Sigma} = \pm \frac{1}{2} \right) &= \sqrt{2m_{\Sigma}} \begin{pmatrix} \chi_{\pm} \\ 0 \end{pmatrix}, \\ \bar{u}_p \left(k, \lambda_p = \pm \frac{1}{2} \right) &= \sqrt{E_p + m_p} \left(\chi_{\pm}^{\dagger}, \frac{\mp |\vec{k}|}{E_p + m_p} \chi_{\pm}^{\dagger} \right), \end{aligned} \quad (\text{B3})$$

where p (k) denotes the four-momentum of the Σ^+ (proton), with $p^0 = m_{\Sigma}$, $|\vec{p}| = 0$ and $E_p = \sqrt{|\vec{k}|^2 + m_p^2}$ is the energy of the proton, hence $k = (E_p, 0, 0, |\vec{k}|)^{\text{T}}$, and $\chi_+ = (1, 0)^{\text{T}}$, $\chi_- = (0, 1)^{\text{T}}$.

Plugging the spinors into (B2) and simplifying, we arrive at

$$\begin{aligned} h_{\frac{1}{2}}^{\Sigma} \left(\lambda_{\Sigma} = \frac{1}{2} \right) &= \sqrt{2m_{\Sigma}} G_F m_{\pi}^2 (\sqrt{r_+} A + \sqrt{r_-} B), \\ h_{-\frac{1}{2}}^{\Sigma} \left(\lambda_{\Sigma} = -\frac{1}{2} \right) &= \sqrt{2m_{\Sigma}} G_F m_{\pi}^2 (\sqrt{r_+} A - \sqrt{r_-} B), \end{aligned} \quad (\text{B4})$$

with $r_{\pm} = \sqrt{E_p \pm m_p}$. Using these helicity amplitudes we can express α_{\pm} as

$$\begin{aligned} \alpha_+ &= 4G_F^2 m_{\pi}^4 m_{\Sigma} (r_+ |A|^2 + r_- |B|^2), \\ \alpha_- &= 8G_F^2 m_{\pi}^4 m_{\Sigma} \sqrt{r_+ r_-} \text{Re}(AB^*), \end{aligned} \quad (\text{B5})$$

and obtain for their ratio

$$\frac{\alpha_-}{\alpha_+} = \frac{2\sqrt{\frac{r_-}{r_+}}\text{Re}(AB^*)}{|A|^2 + \frac{r_-}{r_+}|B|^2} = \alpha, \quad (\text{B6})$$

which corresponds to the decay parameter α in [16]. We can therefore factorize α_+ from the angular distribution and use $\alpha_+ = \mathcal{B}(\Sigma^+ \rightarrow p\pi)$ and $\frac{\alpha_-}{\alpha_+} = \alpha$ to arrive at the expressions given in Sec. II B.

Appendix C: Angular distribution for polarized initial baryons

Taking into account initial state polarization, the differential decay distribution depends on five angles and q^2 and reads

$$\begin{aligned} \frac{d^6\Gamma}{dq^2 d\vec{\Omega}} = \frac{3}{32\pi^2} & \left((K_{1ss} \sin^2 \theta_\ell + K_{1cc} \cos^2 \theta_\ell + K_{1c} \cos \theta_\ell) + \right. \\ & (K_{2ss} \sin^2 \theta_\ell + K_{2cc} \cos^2 \theta_\ell + K_{2c} \cos \theta_\ell) \cos \theta_\pi + \\ & (K_{3sc} \sin \theta_\ell \cos \theta_\ell + K_{3s} \sin \theta_\ell) \sin \theta_\pi \sin (\phi_c + \phi_\ell) + \\ & (K_{4sc} \sin \theta_\ell \cos \theta_\ell + K_{4s} \sin \theta_\ell) \sin \theta_\pi \cos (\phi_c + \phi_\ell) + \\ & (K_{11} \sin^2 \theta_\ell + K_{12} \cos^2 \theta_\ell + K_{13} \cos \theta_\ell) \cos \theta_c + \\ & (K_{14} \sin^2 \theta_\ell + K_{15} \cos^2 \theta_\ell + K_{16} \cos \theta_\ell) \cos \theta_\pi \cos \theta_c + \\ & (K_{17} \sin \theta_\ell \cos \theta_\ell + K_{18} \sin \theta_\ell) \sin \theta_\pi \cos (\phi_c + \phi_\ell) \cos \theta_c + \\ & (K_{19} \sin \theta_\ell \cos \theta_\ell + K_{20} \sin \theta_\ell) \sin \theta_\pi \sin (\phi_c + \phi_\ell) \cos \theta_c + \\ & (K_{21} \cos \theta_\ell \sin \theta_\ell + K_{22} \sin \theta_\ell) \sin \phi_\ell \sin \theta_c + \\ & (K_{23} \cos \theta_\ell \sin \theta_\ell + K_{24} \sin \theta_\ell) \cos \phi_\ell \sin \theta_c + \\ & (K_{25} \cos \theta_\ell \sin \theta_\ell + K_{26} \sin \theta_\ell) \sin \phi_\ell \cos \theta_\pi \sin \theta_c + \\ & (K_{27} \cos \theta_\ell \sin \theta_\ell + K_{28} \sin \theta_\ell) \cos \phi_\ell \cos \theta_\pi \sin \theta_c + \\ & (K_{29} \cos^2 \theta_\ell + K_{30} \sin^2 \theta_\ell) \sin \theta_\pi \sin \phi_c \sin \theta_c + \\ & (K_{31} \cos^2 \theta_\ell + K_{32} \sin^2 \theta_\ell) \sin \theta_\pi \cos \phi_c \sin \theta_c + \\ & (K_{33} \sin^2 \theta_\ell) \sin \theta_\pi \cos (2\phi_\ell + \phi_c) \sin \theta_c + \\ & \left. (K_{34} \sin^2 \theta_\ell) \sin \theta_\pi \sin (2\phi_\ell + \phi_c) \sin \theta_c \right). \end{aligned} \quad (\text{C1})$$

$K_{11}, K_{12}, K_{13}, K_{21}, K_{22}, K_{23}$ and K_{24} survive in the limit $\alpha = 0$ of which K_{13}, K_{22} and K_{24} are null tests. The first four lines are identical to Eq. (5) with $\phi_c + \phi_\ell = \phi$. ϕ_c and θ_c are new

angles related to the initial state polarization, see Ref. [34] for details.

-
- [1] G. Burdman, E. Golowich, J. L. Hewett and S. Pakvasa, Phys. Rev. D **66** (2002), 014009 doi:10.1103/PhysRevD.66.014009 [arXiv:hep-ph/0112235 [hep-ph]].
 - [2] A. Paul, I. I. Bigi and S. Recksiegel, Phys. Rev. D **83** (2011), 114006 doi:10.1103/PhysRevD.83.114006 [arXiv:1101.6053 [hep-ph]].
 - [3] L. Cappiello, O. Cata and G. D'Ambrosio, JHEP **04**, 135 (2013) doi:10.1007/JHEP04(2013)135 [arXiv:1209.4235 [hep-ph]].
 - [4] S. Fajfer and N. Košnik, Eur. Phys. J. C **75** (2015) no.12, 567 doi:10.1140/epjc/s10052-015-3801-2 [arXiv:1510.00965 [hep-ph]].
 - [5] S. de Boer and G. Hiller, Phys. Rev. D **93** (2016) no.7, 074001 doi:10.1103/PhysRevD.93.074001 [arXiv:1510.00311 [hep-ph]].
 - [6] S. De Boer and G. Hiller, Phys. Rev. D **98** (2018) no.3, 035041 doi:10.1103/PhysRevD.98.035041 [arXiv:1805.08516 [hep-ph]].
 - [7] R. Bause, M. Golz, G. Hiller and A. Tayduganov, Eur. Phys. J. C **80** (2020) no.1, 65 doi:10.1140/epjc/s10052-020-7621-7 [arXiv:1909.11108 [hep-ph]].
 - [8] H. Gisbert, M. Golz and D. S. Mitzel, Mod. Phys. Lett. A **36** (2021) no.04, 2130002 doi:10.1142/S0217732321300020 [arXiv:2011.09478 [hep-ph]].
 - [9] S. Meinel, Phys. Rev. D **97** (2018) no.3, 034511 doi:10.1103/PhysRevD.97.034511 [arXiv:1712.05783 [hep-lat]].
 - [10] R. Bause, H. Gisbert, M. Golz and G. Hiller, Phys. Rev. D **103**, no.1, 015033 (2021) doi:10.1103/PhysRevD.103.015033 [arXiv:2010.02225 [hep-ph]].
 - [11] G. Faisel, J. Y. Su and J. Tandean, JHEP **04**, 246 (2021) doi:10.1007/JHEP04(2021)246 [arXiv:2012.15847 [hep-ph]].
 - [12] M. Golz, G. Hiller and T. Magorsch, JHEP **09**, 208 (2021) doi:10.1007/jhep09(2021)208 [arXiv:2107.13010 [hep-ph]].
 - [13] G. Hiller and A. Kagan, Phys. Rev. D **65**, 074038 (2002) doi:10.1103/PhysRevD.65.074038 [arXiv:hep-ph/0108074 [hep-ph]].
 - [14] T. Gutsche, M. A. Ivanov, J. G. Korner, V. E. Lyubovitskij and P. Santorelli, Phys. Rev. D **87** (2013), 074031 doi:10.1103/PhysRevD.87.074031 [arXiv:1301.3737 [hep-ph]].
 - [15] P. Böer, T. Feldmann and D. van Dyk, JHEP **01** (2015), 155 doi:10.1007/JHEP01(2015)155 [arXiv:1410.2115 [hep-ph]].
 - [16] P. A. Zyla *et al.* [Particle Data Group], PTEP **2020** (2020) no.8, 083C01 doi:10.1093/ptep/ptaa104
 - [17] R. N. Faustov and V. O. Galkin, Eur. Phys. J. C **78** (2018) no.6, 527 doi:10.1140/epjc/s10052-018-6010-y [arXiv:1805.02516 [hep-ph]].

- [18] K. Azizi, Y. Sarac and H. Sundu, Eur. Phys. J. A **48**, 2 (2012) doi:10.1140/epja/i2012-12002-1 [arXiv:1107.5925 [hep-ph]].
- [19] R. Aaij *et al.* [LHCb], Phys. Rev. D **97** (2018) no.9, 091101 doi:10.1103/PhysRevD.97.091101 [arXiv:1712.07938 [hep-ex]].
- [20] J. P. Lees *et al.* [BaBar], Phys. Rev. D **84**, 072006 (2011) doi:10.1103/PhysRevD.84.072006 [arXiv:1107.4465 [hep-ex]].
- [21] A. Cerri, V. V. Gligorov, S. Malvezzi, J. Martin Camalich, J. Zupan, S. Akar, J. Alimena, B. C. Allanach, W. Altmannshofer and L. Anderlini, *et al.* CERN Yellow Rep. Monogr. **7** (2019), 867-1158 doi:10.23731/CYRM-2019-007.867 [arXiv:1812.07638 [hep-ph]].
- [22] E. Kou *et al.* [Belle-II Collaboration], PTEP **2019**, no. 12, 123C01 (2019) [arXiv:1808.10567 [hep-ex]].
- [23] M. Ablikim *et al.*, Chin. Phys. C **44** (2020) no.4, 040001 [arXiv:1912.05983 [hep-ex]].
- [24] A. E. Bondar *et al.* [Charm-Tau Factory], Phys. Atom. Nucl. **76** (2013), 1072-1085 doi:10.1134/S1063778813090032
- [25] A. Abada *et al.* [FCC Collaboration], Eur. Phys. J. C **79**, no. 6, 474 (2019).
- [26] S. Fajfer and S. Prelovsek, Phys. Rev. D **73**, 054026 (2006) doi:10.1103/PhysRevD.73.054026 [arXiv:hep-ph/0511048 [hep-ph]].
- [27] S. X. Li *et al.* [Belle], Phys. Rev. D **104**, no.7, 072008 (2021) doi:10.1103/PhysRevD.104.072008 [arXiv:2108.11301 [hep-ex]].
- [28] N. Adolph and G. Hiller, in preparation.
- [29] R. Chistov *et al.* [Belle], Phys. Rev. D **88** (2013) no.7, 071103 doi:10.1103/PhysRevD.88.071103 [arXiv:1306.5947 [hep-ex]].
- [30] S. de Boer, Eur. Phys. J. C **77** (2017) no.11, 801 doi:10.1140/epjc/s10052-017-5364-x [arXiv:1707.00988 [hep-ph]].
- [31] S. de Boer, <http://hdl.handle.net/2003/36043>. PhD thesis. Technische Universität Dortmund, 2017.
- [32] H. E. Haber, [arXiv:hep-ph/9405376 [hep-ph]].
- [33] J. Gratrex, M. Hopfer and R. Zwicky, Phys. Rev. D **93** (2016) no.5, 054008 doi:10.1103/PhysRevD.93.054008 [arXiv:1506.03970 [hep-ph]].
- [34] T. Blake and M. Kreps, JHEP **11** (2017), 138 doi:10.1007/JHEP11(2017)138 [arXiv:1710.00746 [hep-ph]].
- [35] G. Hiller and R. Zwicky, JHEP **11**, 073 (2021) doi:10.1007/JHEP11(2021)073 [arXiv:2107.12993 [hep-ph]].
- [36] S. de Boer and G. Hiller, JHEP **08**, 091 (2017) doi:10.1007/JHEP08(2017)091 [arXiv:1701.06392 [hep-ph]].
- [37] E. D. Commins and P. H. Bucksbaum, Cambridge University Press (1983) isbn: 978-0-521-27370-1.